

"Realization of high-temperature superconductivity in nano-carbon materials and its power application"

12/08/2012

Name of Principal Investigators:

- e-mail address : J-haru@ee.aoyama.ac.jp
- Institution : Aoyama Gakuin University
- Mailing Address : 5-10-1 Fuchinobe, Sagamihara, Kanagawa 252-5258 Japan
- Phone : +81-42759-6256
- Fax : +81-42759-6524

Period of Performance: 1/08/2011 – 31/07/2012

Abstract: Nano-carbon materials (carbon nanotubes (CNTs) and graphenes) are attracting significant attention. In particular, they have possibility for realization of high-transition temperature (T_c) superconductivity (SC) (*e.g.*, $T_c > 40\text{K}$). In the present work, I have tried to fabricate the following two novel-type CNT-based samples and measured those magnetizations. (1) Thin films of assembled sulfur-doped multi-walled CNTs (MWNTs), (2) Arrays of boron-doped MWNTs synthesized on SiC substrate. We find that the former exhibits Meissner effect with the highest T_c of 22K similar to that in boron-doped CNTs. This T_c value is the highest in carbon materials except for fullerene-based SC. It is, however, instable and reproducibility is poor. Thus, improvement of sulfur doping method is indispensable. In contrast, the latter exhibits magnetization drop with T_c as high as 35K. However, it was not identified as SC.

Furthermore, I have also fabricated graphene-based samples (the so-called graphene nanomeshes with honeycomb-like arrays of hydrogen-terminated nano pores) and find presence of polarized electron spins at the pore edges and ferromagnetism. It must produce SC by no-termination or different foreign-atom termination of the edge dangling bonds in near future.

Introduction: SC is very attractive issue for any societies and people. Various kinds of superconductors have been discovered so far; *e.g.*, CuO_2 -based SC with high- T_c over 100K, SC metals (*e.g.*, MgB_2 with T_c of 40K), organic SCs. Here, CNTs are nano-sized diameter tubes consisting of carbon atoms. After its discovery by Dr. Sumio Iijima at 1991, various unique structures, electronic states, and quantum phenomena have been reported. Application of CNTs is also actively studied. However, reports of SC in CNTs were only a few. Previously, I obtained (1) SC in entirely end-bonded MWNTs with the world-highest T_c of 12K and (2) SC in thin films of boron-doped single-walled CNTs (SWNTs) with $T_c = 12\text{K}$. Moreover, based on this grant in last year, I found possible $T_c = 28\text{K}$ in thin films of boron-doped SWNTs. However, I could not yet conclude this T_c as SC from some reasons (*e.g.*, poor reproducibility and instability). Moreover, CNTs should provide much higher T_c , which is originated from high phonon-frequency of carbon atoms, extremely high electronic density of states (EDOSs) in van Hove singularities (VHSs) of one-dimensional system, and strong electron-phonon coupling between radial breathing phonon mode and σ - π electrons. Hence, we have continuously carried out fabrication of novel-type CNTs and explored higher T_c with high reproducibility.

As the other novel material, graphene is attracting significant attention. Graphene is an ultimate two-dimensional molecule film with thickness as thin as only one carbon atom size. Because the novel fabrication method was found at 2004 and a variety of interesting phenomena has been report as well as those applications, Graphene got Nobel Prize at 2010.

Report Documentation Page			Form Approved OMB No. 0704-0188		
Public reporting burden for the collection of information is estimated to average 1 hour per response, including the time for reviewing instructions, searching existing data sources, gathering and maintaining the data needed, and completing and reviewing the collection of information. Send comments regarding this burden estimate or any other aspect of this collection of information, including suggestions for reducing this burden, to Washington Headquarters Services, Directorate for Information Operations and Reports, 1215 Jefferson Davis Highway, Suite 1204, Arlington VA 22202-4302. Respondents should be aware that notwithstanding any other provision of law, no person shall be subject to a penalty for failing to comply with a collection of information if it does not display a currently valid OMB control number.					
1. REPORT DATE 17 SEP 2012		2. REPORT TYPE Final		3. DATES COVERED 14-07-2011 to 13-07-2012	
4. TITLE AND SUBTITLE Realization of High-Temperature Superconductivity in Nano Carbon Materials and Their Power Application			5a. CONTRACT NUMBER FA23861114093		
			5b. GRANT NUMBER		
			5c. PROGRAM ELEMENT NUMBER		
6. AUTHOR(S) Junji Haruyama			5d. PROJECT NUMBER		
			5e. TASK NUMBER		
			5f. WORK UNIT NUMBER		
7. PERFORMING ORGANIZATION NAME(S) AND ADDRESS(ES) Aoyama Gakuin University,5-10-1 Fuchinobe, Sagamihara,Kanagawa 229-8558,Japan,NA,NA			8. PERFORMING ORGANIZATION REPORT NUMBER N/A		
9. SPONSORING/MONITORING AGENCY NAME(S) AND ADDRESS(ES) AOARD, UNIT 45002, APO, AP, 96338-5002			10. SPONSOR/MONITOR'S ACRONYM(S) AOARD		
			11. SPONSOR/MONITOR'S REPORT NUMBER(S) AOARD-114093		
12. DISTRIBUTION/AVAILABILITY STATEMENT Approved for public release; distribution unlimited					
13. SUPPLEMENTARY NOTES					
14. ABSTRACT Nano-carbon materials (carbon nanotubes (CNTs) and graphenes) are attracting significant attention. In particular, they have possibility for realization of high- transition temperature (Tc) superconductivity (SC) (e.g., Tc > 40K). In the present work, the researchers have tried to fabricate the following two novel-type CNT-based samples and measured those magnetizations: (1) Thin films of assembled sulfur-doped multi-walled CNTs (MWNTs), and (2) Arrays of boron-doped MWNTs synthesized on SiC substrate. They find that the former exhibits Meissner effect with the highest Tc of 22K similar to that in boron-doped CNTs. This Tc value is the highest in carbon materials except for fullerene-based SC. It is, however, instable and reproducibility is poor.					
15. SUBJECT TERMS Carbon nano tubes, Superconducting Materials					
16. SECURITY CLASSIFICATION OF:			17. LIMITATION OF ABSTRACT Same as Report (SAR)	18. NUMBER OF PAGES 8	19a. NAME OF RESPONSIBLE PERSON
a. REPORT unclassified	b. ABSTRACT unclassified	c. THIS PAGE unclassified			

However, there is one issue, which mostly none reported experimentally. That's edge-based phenomena. Zigzag atomic structure of graphene edges has a flat energy band, resulting in electron localization and those spontaneous spin polarization. It is highly expected that the polarized spins produce high- T_c SC. Thus, we have fabricated novel edge system of graphenes (i.e., low-defect graphene nanomeshes with honey-comb like array of hexagonal nanopores) and explored SC by terminating the pore edge atoms by foreign atoms (e.g., hydrogen, oxygen, boron).

Experiments:

Two CNT-based systems:

(1) Thin films of assembled sulfur-doped MWNTs (S-MWNTs),

These were synthesized by CVD growth of MWNTs with mixing sulfur gas. After the synthesis, high quality of the S-MWNTs was confirmed by Raman spectroscopy. Then, they were centrifuged in order to exclude impurities and also ultra-sonication was carried out in order to resolve the ropes of MWNTs to individual one. After then, the S-MWNTs dispersed on Si substrate uniformly by using spin coating, resulting in highly uniform thin film of the assembled S-MWNTs.

(2) Arrays of boron-doped MWNTs (B-MWNTs) synthesized on SiC substrate.

These were synthesized by thermal resolution of SiC surface.

Magnetization of both the samples were measured by superconducting quantum interference devices (SQUID; Quantum designs).

Graphene nanomeshes:

Low-defect graphene nanomeshes with honeycomb-like arrays of hexagonal nanopores were fabricated on a large ensemble of mechanically exfoliated graphenes by non-lithographic method using a nanoporous alumina template (NPAT). Using the NPAT as a mask, assembled graphenes were etched by a carefully optimized conditions using low-power Ar gas to avoid giving damage to the nanopore edges. The nanopore edges are not intentionally aligned along the hexagonal carbon lattice of graphene in this process. After formation of the nanomesh on graphenes, the NPAT mask was entirely dissolved by a H_3PO_4 solution (or detached mechanically from the graphene nanomeshes in some cases). It left no contamination.

All the graphene nanomeshes fabricated through these processes were annealed at 800 °C in high vacuum (10^{-6} Torr) for 0.5 - 3 days and then in hydrogen gas for 1-3 hours for all the measurements. The first annealing is for deoxidization of the pore edges and recovering all damages, while the second annealing is for termination of the carbon atoms at the pore edges by hydrogen atoms. These annealing processes also give the pore edge states high chemical stability.

Results and Discussion:

Thin films of S-MWNTs:

Scanning Electron Microscope (SEM) top-view image of a thin film consisting of the assembled S-MWNTs is shown in Fig.1. It exhibits highly uniform film structure. Typical measurement result of magnetization of the thin films of S-MWNTs is shown in Fig.2. Temperature dependence of magnetization (Fig.2(a)) shows gradual magnetization drop to negative magnetization regions starting from $T_c \sim 22$ K in both zero-field and field cooling (ZFC and FC) regimes. Figure 2(b) shows magnetic field dependence of magnetization at $T = 4$ K. It exhibits diamagnetism with small magnitude of a hysteresis loop. These can be strong evidence for Meissner effect. However, the features have also poor reproducibility and instability. That's similar to the case of possible $T_c = 28$ K in thin films of B-SWNTs, which we found in last year.

Previous one work reported that S-graphites exhibited T_c as high as over 35 K. MWNTs have a structure of rolled-up graphites. That is why I have used S-MWNTs for the present experiment. The S-MWNTs actually showed high- T_c SC as mentioned above. The poor reproducibility is also quite similar to the case of S-graphites. It may be due to instable chemical-bonds between S and carbon atoms. Therefore, improvement of S-doping is indispensable.

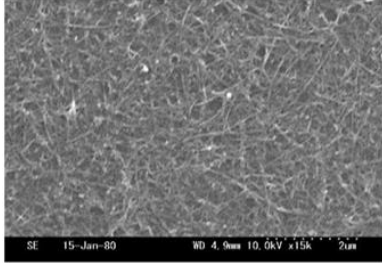


Fig. 1

Fig.1: SEM top-view image of a thin film consisting of sulfur-doped MWNTs. It exhibits high uniformity. The samples were provided from Clemson University, Prof.Rao's group.

Fig.2(a): Temperature dependence of magnetization of Fig.1 -sample. It shows gradual magnetization drops due to Meissner effect starting from $T_c \sim 22$ K in both zero-field and field cooling (ZFC and FC) regimes.

Fig.2(b): Magnetic field dependence of magnetization at $T = 4$ K. It exhibits diamagnetism with small magnitude of a hysteresis loop due to Meissner effect.

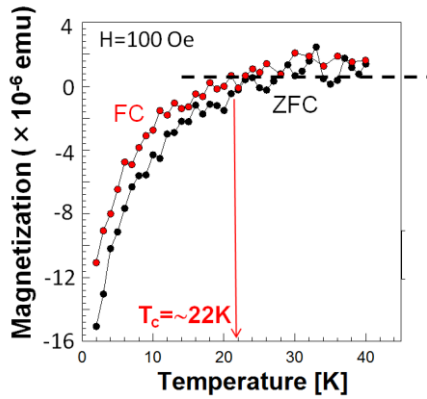


Fig. 2(a)

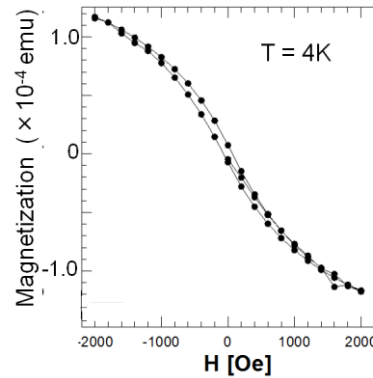


Fig. 2(b)

Arrays of B-MWNTs:

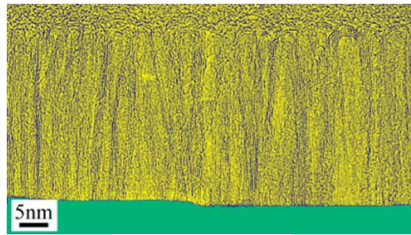


Fig. 3

Fig.3: Cross-sectional TEM image of array of boron-doped MWNTs fabricated by thermal dissolution of SiC substrate. The samples were provided from Nagoya University, Prof. Kusunoki group.

Fig.4(a): Temperature dependence of magnetization of Fig.3 -sample. It shows a gradual magnetization drop starting from $T_c \sim 35$ K only in ZFC regime.

Fig.4(b): Magnetic field dependence of magnetization at $T = 10$ K. It exhibits diamagnetism with small magnitude of a hysteresis loop.

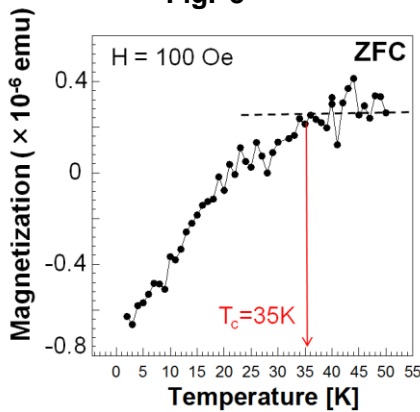


Fig. 4(a)

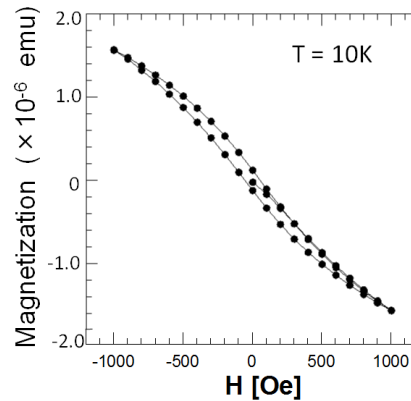


Fig. 4(b)

Figure 3 shows a cross-sectional TEM image of array of B-MWNTs fabricated by thermal dissolution of SiC substrate. Figure 4(a) shows temperature-dependence of magnetization of arrays of B-MWNTs in ZFC regime. It also exhibits a gradual magnetization drop from T_c as high as 35 K. Small-magnitude diamagnetism at $T = 10$ K is also shown in Fig.4(b). However, in the case, no magnetization drop is observed in FC regime. Thus, the results in Fig.4 cannot be concluded as Meissner effect.

As mentioned in introduction, B-SWNTs exhibited Meissner effect. However, one-dimensionality (1D) of the SWNTs obstructed emergence of stable SC. Thus, in the present experiment, I have used arrays of B-MWNTs, because the structure can suppress 1D of SWNTs due to inter-wall(layer) coupling and also inter tube coupling. The reason why Meissner effect was not observed may be because the suppression of 1D prevented appearance of SC, which comes from strong electron-phonon interaction and VHSs.

Graphene nanomeshes:

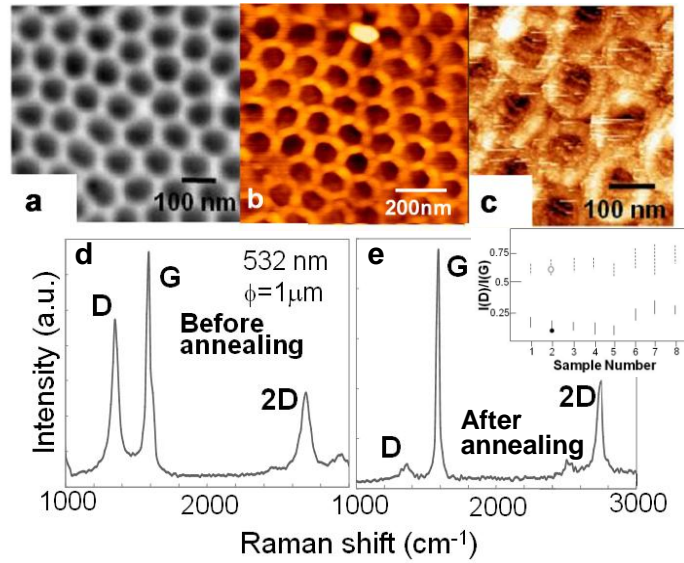


Fig. 5. (a) SEM image of nano-porous alumina template (NPAT) with mean pore diameter $\phi \sim 80$ nm and mean interpore spacing $W \sim 20$ nm (i.e., W corresponds to the graphene nanoribbon width). (b) AFM image of a graphene nanomesh formed by using (a) as an etching mask, which proves hexagonal shape of nanopores. (c) STM image of the approximately 10-layer graphene nanomesh obtained at 80 K in constant-current mode. Lighter regions at pore edges denote higher EDOS and possibly suggest presence of the zigzag pore edges. (d)(e) Typical Raman spectra of a graphene nanomesh (d) prior and (e) after annealing at 800 °C, taken with a laser excitation of 532 nm and 0.14 mW incident power at room temperature. $I(D)/I(G)$ value is drastically reduced by annealing. Because the laser beam diameter ϕ used for the measurement is 1 μ m, the result reflects edge information of ~ 60 pores. **Inset of (e)** Distribution of $I(D)/I(G)$ in eight samples. Fifteen points at five different positions were observed per sample. Dotted and solid lines above and below 0.5 denote $I(D)/I(G)$ prior and after annealing, respectively. Black and open symbols correspond to main panels of Figs. 5(d) and 5(e), respectively.

Figure 5(a) shows SEM image of a NPAT. It exhibits honeycomb-like array of hexagonal nanopores with high regularity. AFM image of the fabricated graphene nanomesh, which also exhibits honeycomb like array of hexagonal nanopores, is shown in Fig.5(b). It shows that nanomesh of the NPAT is successfully transferred on graphene. Figure 5(c) shows scanning tunnel microscope (STM) image of the graphene nanomesh with hydrogen termination of the pore edges. It suggests possible presence of high electronic density of states at pored edges. Figures 5(d) and 5(e) shows Raman spectrum of the nanomesh before and after high-temperature annealing. We find that after the annealing, D-peak

height is strongly suppressed. This can be strong evidence for presence of zigzag atomic structure at the nanopore edges from the following two reasons. **(1)** Singapore group reported that this is because the double resonance process, which induces D peak, can be fulfilled only at an armchair edge when the one-dimensional character of the edge is considered. Indeed, it exhibited $I(D)/I(G)$ value < 0.1 for observation of zigzag edge of graphene flakes by using angle-dependent Raman spectroscopy with polarized laser beam. It is qualitatively consistent with Fig.1e. **(2)** The low $I(D)$ values are also qualitatively consistent with German group's report for graphene nanomeshes, whose hexagonal-pore boundaries are intentionally aligned along the carbon hexagonal lattice by specified method, resulting in formation of the pure zigzag pore edges. Moreover, MIT group suggested that Joule heating of a mixture of zigzag and armchair edges in graphitic nanoribbons reconstructs towards mostly zigzag edges. In our system, we argue that high-temperature (800 °C) annealing for narrow (~ 20 nm) GNRs can play the role similar to that of Joule heating. We reconfirmed that only the samples with showing the low $I(D)$ values can exhibit ferromagnetism.

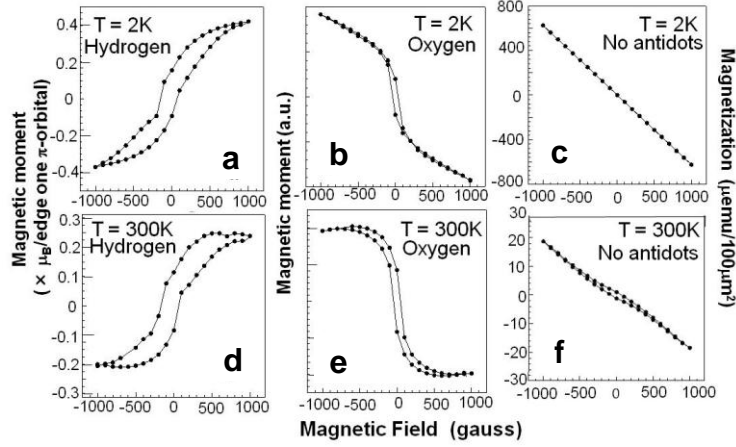


Fig. 6. Magnetization of monolayer graphene nanomeshes with $\phi \sim 80$ nm and $W \sim 20$ nm for (a)(d) hydrogen-terminated edges; (b)(e) oxygen-terminated nanopore edges; and (c)(f) bulk graphene without nanopore arrays. DC magnetization was measured by a superconducting quantum interference device (SQUID; Quantum Design) at 2 K and at room temperature for panels (a)–(c) and panels (d)–(f) respectively. Magnetic fields were applied perpendicular to graphene nanomeshes. The vertical axes in panels (a) and (d) denote magnetic moment per localized-edge π orbital, assuming mono-hydrogenation of individual edge carbon atoms. For Fig.6(d), difference in magnetic moment between upper and lower curves of hysteresis loop at $H = 0$ (residual magnetization $B_r \times 2$) is $\sim 0.2 \mu_B$ and the loop width at zero magnetic moment (coercivity $H_c \times 2$) is ~ 260 gauss.

Figure 6 shows typical results of magnetization measurements. Figure 6(a) shows a magnetization curve for the hydrogen(H)-terminated graphene nanomesh at 2 K. A ferromagnetic-hysteresis loop with large amplitude is clearly observed. In contrast, this feature becomes a diamagnetism-like weak hysteresis loop for oxygen-terminated nanomesh (Fig. 6(b)). Bulk graphenes without nanopores and those assembled with alumina template show mostly no such features even after H_2 annealing (Figs. 6(c) and 6(f)), implying That no parasitic factors (e.g., defects, impurities) of bulk graphenes contribute to the ferromagnetism. It is also confirmed that the features observed at 2 K appear even at room temperature with a larger magnitude of the hysteresis loops (Figs. 6(d–f)), although the amplitude of magnetization decreases.

For reconfirmation of correlation of the observed ferromagnetism with the zigzag pore edge, we performed magnetic force microscope (MFM) observations (Fig.7). The interpore regions, which correspond to GNRs, exhibit mostly uniform darker color that means higher density of polarized spins, in all parts. This suggests that the observed ferromagnetism is

attributed not to defects(disorder), which exists at random, but to all interpore GNR regions, although poor resolution does not allow direct observation of edge-localized spins. In particular, the parts indicated by two arrows evidently imply contribution of the pore edges to ferromagnetism.

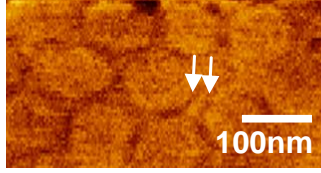


Fig. 7. Magnetic force microscope (MFM) images of an H-terminated graphene nanomeshes on SiC substrate, which showed ferromagnetism similar to Fig.6. CoPtCr-coated Si probe was used for the measurements with a tapping mode. Darker colors mean higher density of polarized spins. In particular, the parts indicated by two arrows evidently imply pore edge lines.

These results imply the presence of polarized spins with ferromagnetic configuration at the pore edges. This has been for the first time observed. However, it is highly sensitive to foreign atoms terminating the zigzag edges. Indeed, oxygen-terminated pore edges exhibited diamagnetism. This can be a signature of Meissner effect. Moreover, it is theoretically well known that graphene zigzag edges without any foreign-atom termination exhibit anti-ferromagnetism, which also leads to Meissner effect at consequent low energy (e.g., low temperature and low bias voltages). This edge state can be realized in high vacuum. Therefore, it is highly expected that the observed ferromagnetism and diamagnetism must lead to Meissner effect in near future.

Conclusion

I fabricated the following two novel-type CNT-based samples and measured those magnetizations. (1) Thin films of assembled S-MWNTs, (2) Arrays of B-MWNTs synthesized on SiC substrate. We found that the former exhibited Meissner effect with the highest T_c of 22K similar to that in B-CNTs. However, it was instable and the reproducibility of SC was poor. Improvement of sulfur doping method is indispensable. In contrast, the latter exhibited magnetization drop with T_c as high as 35K. It was, however, not identified as SC, because it showed no magnetization drop in FC regime of the temperature dependence.

Moreover, I also fabricated graphene nanomeshes with the honeycomb-like arrays of hydrogen-terminated nanopores and found presence of polarized electron spins at the pore edges and consequent spontaneous appearance of ferromagnetism. It is highly expected that it must produce SC by no-termination or different foreign-atom termination of the edge dangling bonds in near future.

List of Publications:

1. T.Shimizu, **J.Haruyama**, D. C.Marcano, D. V. Kosynkin, J.M.Tour, K.Hirose, K.Suenaga, "Large intrinsic energy bandgaps in annealed nanotube-derived graphene nanoribbons" **Nature Nanotechnology** 6, 45-50 (2011)
(Selected for Latest Highlights, News & Views, Cover index)
2. K. Tada, **J. Haruyama**, H. Yang, M. Chshiev, T. Matsui, H. Fukuyama, "Ferromagnetism in hydrogenated graphene nanopore arrays", **Phys. Rev. Lett.** 107, 217203 (2011.11 – 2012.3)
3. T. Shimizu, J. Nakamura, K. Tada,Y. Yagi, **J. Haruyama** , "Magnetoresistance oscillations arisen from edge-localized electrons in low-defect graphene antidot-lattices", **Appl.Phys.Lett.** 100, 023104 (2012)
4. K. Tada, **J. Haruyama**, H. Yang, M. Chshiev, "Spontaneous spin polarization and spin pumping effect at edges of graphene antidot lattices" *Physica Status Solidi (b)* (2012) **In printing**
5. K. Tada, T. Hasegawa, **J. Haruyama**, H. Yang, M. Chshiev, "Edge related spin polarization and anomalous magnetoresistance in graphene nanopore arrays" *Journal of superconductivity and novel magnetisms* (2012) **In printing**
6. **J.Haruyama**, "Magnetism and spintronics arising from Graphene edges" in "**Innovative Graphene Technologies: Developments, Characterization and Evaluation**", Rapra-Smithers Publication (2012) **In printing**
7. **J.Haruyama**, "Magneism and spintronics in Graphenes" in "Recent advancement of Graphenes", American Nano Society (2012) **In printing**
8. K. Tada, **J. Haruyama**, H. Yang, M. Chshiev, T. Matsui, H. Fukuyama, "Graphene magnets derived from pore-edge electrons in low-defect graphene nanopore arrays", **Journal of Nanoresearch** (2012) **In printing**
9. **J.Haruyama**, "Superconductivity in carbon nanotubes and its application to spin quantum bits", in "**Superconductivity Research Advances**" (Nova Science Publishers, Inc 2012) **In printing**
10. **J.Haruyama**, "Superconductivity in carbon nantoubes" in "**Carbon-based new superconductors; Toward high T_c** " edited by **J. Haruyama** (Pan Stanford Publishing, Singapore 2012) **In printing (Editor)**

Invited talks

1. "Spin-related phenomena and application to spintorronics in graphenes", The 2nd Annual World Congress of Nano-Science &Technology, Beijing, China (October, 2012)
2. "Graphene magnets and spintronics arising from graphene edges", The 5th Szeged International Workshop on Advances in Nanoscience,Szedo, Hungary (October, 2012)
3. "Superconductivity and spintronics in nano-carbon materials", Colloquium at Dept.Physics, Sorbonne Universite (Universite of Marie Curie) (September 2012)
4. "Graphene edges: Physics and applications", C2C Workshop: Progress in Nanoscience and Materials, Shanghai (August 2012)
5. "Magnetism and spintronics arising from graphene edges", 4th Worldwide Universities Network (WUN) International Conference on SpintronicsSydney, Australia (July 2012)
6. "Spintronics in graphene edges" The 1st Annual World Congress of Advanced-Material 2012, Beijing, China (June 2012)

7. "Magnetism and spintronics arising from graphene edges"
International Conference on Superconductivity and Magnetism, Istanbul, Turkey (April 2012)
8. "Edge-related magnetism and spintronics in graphenes",
26th International Winter school on Electronic Properties of Novel Materials, Kirchberg, Austria (March, 2012)
9. "Physics and application of graphene edges: Nanoribbons and Nanopore arrays"
The 2nd A3 Symposium of Emerging Materials, China (October 2011)
10. "Large intrinsic band gaps and ferromagnetism derived from edge states: Graphene Nanoribbons and Antidot-lattice Graphenes",
The 1st Annual World Congress of Nano-Science & Technology, Dalian, China (October, 2011)
11. "Physics and application of graphene edges: Graphene nanoribbons and Graphene nanopore arrays"
International Conference on Nanoscience and Technology, Beijing, China (September 2011)

DD882: As a separate document, please complete and sign the inventions disclosure form.